Supporting Information for "The Global Distribution and Drivers of Grazing Dynamics Estimated from Inverse Modelling"

Tyler Rohr[1,2], Anthony Richardson[3,4], Andrew Lenton[5], Matt Chamberlain[5],

Elizabeth Shadwick[2,5]

[2]Institute for Marine and Antarctic Science, University of Tasmania, Hobart, Tasmania, 7000, Australia

[2]Australian Antarctic Partnership Program, Hobart, Tasmania, 7000, Australia

[3]School of Environment, 4072, The University of Queensland, St Lucia, Queensland, Australia

[4]Commonwealth Scientific and Industrial Research Organisation (CSIRO) Environment, BioSciences Precinct (QBP), St Lucia,

Queensland, 4067, Australia

[5]Commonwealth Scientific and Industrial Research Organisation (CSIRO) Environment, Hobart, Tasmania, 7000 Australia

Contents of this file

1. Supporting Text 1 to 3

2. Supporting Figures 1 to 4

3. Supporting Table 1

———

Corresponding author: Tyler Rohr, Australian Antarctic Partnership Program, Hobart, Tasmania, 7000, Australia. (tyler.rohr@utas.edu.au)

May 10, 2023, 6:05am

Supporting Text 1. Distribution and drivers of grazing dynamics using the VIIRS chlorophyll record

In **Figure 1** we use phytoplankton carbon biomass estimated remotely from the Carbon-based Productivity Model (Westberry et al., 2008) to compare directly to prognostic phytoplankton biomass resolved in the simulation. However, estimating carbon biomass from space using particle back-scattering involves a different set of assumptions than traditional estimates of phytoplankton abundance which infer chlorophyll concentrations from ocean color. To confirm these differences did not influence our results we repeated the analysis comparing the seasonal cycle of modelled phytoplankton carbon to that of remotely sensed chlorophyll from VIIRS (Sathyendranath et al., 2019). The results were largely consistent (**Supporting Figure 1**).

The primary difference is that the two clear asymptotes apparent when using CbPM biomass as an indicator of phytoplankton abundance are now not as well defined, with the lower asymptote disappearing entirely. Note, while we use a sigmoidal function to fit the relationship for consistency and direct comparison, it may be better described with a rect-angular hyperbole. It is not entirely clear why there is no lower asymptote for chlorophyll but it may have to do with the detection threshold for ocean colour versus backscatter, the fact that at low phytoplankton concentrations the particle back scatter signal may no longer be dominated by phytoplankton, or variability in the carbon to chlorophyll ratio as a result of community composition or photo-adaptation. Never the less, our two most important results remain consitent: 1. The type III response consistently outperforms the type II response (**Supporting Figure 2, Supporting Table 1**) and 2. the seasonal

May 10, 2023, 6:05am

cycle in more eutrophic regions is better described using larger $K_{1/2}$ values (**Supporting Figures 1, 2**)

Note, model skill scores appear higher for VIIRS than CbPM (**Supporting Table 1**); however, model skill was normalized across all runs using chlorophyll (VIIRS) and all run using carbon (CbPM) independently. Thus, the higher scores for VIIRS do not necessarily mean the modelled seasonal phytoplankton cycle better reflects observed chlorophyll compared to carbon, but rather that the difference between the model skill achieved with the optimal $K_{1/2}$ values compared to sub-optimal $K_{1/2}$ values is larger when comparing to observed chlorophyll.

Supporting Text 2. First order stability of the functional response

The shape of the functional response curve, $g([C_{phyto}])$, influences the shape of the seasonal cycle of phytoplankton biomass primarily through its stabilizing or destabilizing influence on phytoplankton population dynamics (Gentleman & Neuheimer, 2008). The stabilizing influence of grazing is determined by how clearance rates ($Cl = g([C_{phyto}])/[C_{phyto}]$) change in response to changing phytoplankton biomass. If phytoplankton accumulation decreases clearance rates, thereby promoting further population growth, that is a positive feed back with a destabilizing influence. Alternatively, if phytoplankton accumulation increases clearance rates, thereby damping further population growth, that is a negative feed back with stabilizing influence. The stabilizing influence of the functional response at a given phytoplankton concentration can thereby be quantified by the first derivation of the clearance rate with respect to the phytoplankton concentration (i.e. $\frac{dCl}{d[C_{phyto}]}$). The value of $\frac{dCl}{d[C_{phyto}]}$ is determined both the shape of $g([C_{phyto}])$ as

well as the prognostic phytoplankton concentration which determines where on the curve $\frac{dCl}{d[C_{phyto}]}$ is evaluated.

To capture a mean sense of the stabilizing influence of the functional response across a complete model run and many different phytoplankton concentrations, we define the mean first order stability as the value of $\frac{dCl}{d[C_{phyto}]}$ at the mean annual $[C_{phyto}]$ in a given grid cell of a given run. The mean first order stability of our experiments was consistently negative (destabilizing) when a type II response was employed (**Figure S3B**) and positive (stabilizing) when a type III response was employed (**Figure S3A**). Note, while it is not possible to have positive first order stability when a type II response is used, it is possible to have negative first order stability stability when a type III response is used. The latter is possible in model configurations with a very low g_{max} or very strong bottom-up growth conditions that could buoy phytoplankton populations above $K_{1/2}$.

Regardless of response type, large $K_{1/2}$ values stretch out the response curve, leading to the depression and linearization of the functional response at low (but common) prey concentrations, slow and steady clearance rates, and very little influence on the stability of the system. Decreasing $K_{1/2}$ with a type II response monotonically decreases the first order stability by both directly altering the shape of the functional response curve and indirectly decreasing the prognostic phytoplankton population via increased grazing pressure. Decreasing $K_{1/2}$ with a type III response monotonically increases the first order stability of the system. This occurs because decreasing $K_{1/2}$ increases grazing pressure and, without suitably strong bottom-controls, keeps the annually-averaged phytoplankton concentration below $K_{1/2}$, where the first order stability increases as $K_{1/2}$ decreases.

Supporting Text 3. Challenges and potential of parameterizing zooplankton community composition

By invoking the equations descried in **Figure 1** or **Supporting Table 1** modellers could implicitly resolve changes in zooplankton community composition by driving changes in the community-integrated functional attributes (i.e. $K_{1/2}$) of a single zooplankton group with changes in prey abundance. However, experimenting with this parameterization warrants careful consideration of several factors.

Ecologically, such a parameterization requires assuming that a) bulk phytoplankton biomass co-varies with phytoplankton community composition in a systematic way, with less productive waters inhabited by smaller phytoplankton (Roy et al., 2013), and b) zooplankton community composition is determined by the composition of the prey field in a systematic way, with more efficient grazing able to dominate when prey options are smaller (Kiørboe & Hirst, 2014). While both assumptions are generally well supported by observations and together are consistent with the emergent relationship between observed phytoplankton biomass and the inferred grazing dynamics required to best recreate its seasonal cycle (**Figure 1**), implementing the associated relationship introduces additional challenges.

First off, the specific parameters listed in **Supporting Table 1** and **Figure 1** would likely need to be tuned-up to the bottom-up configuration and physical dynamics of each particular model in which they are embedded. Secondly, it is not obvious what space and time scales one should assume that specific grazing rates should change due to the influence of food scarcity on individual zooplankton versus the influence of zooplankton community

composition on mean grazing dynamics. That is, while the value of $K_{1/2}$ determines the instantaneous response of zooplankton grazing rates to food scarcity, it should take longer for $K_{1/2}$ itself to evolve. This is because $K_{1/2}$ reflects the mean physiological characteristics of the entire zooplankton community and can only change at the rate with which community composition can evolve. This timescale likely varies globally and as a function of other environmental drivers such as temperature (Richardson, 2008). For example, much shorter time periods are needed in communities dominated by asexually-reproducing zooplankton such as salps compared to those dominated by zooplankton with complex, multi-year, life histories, such as euphausiids (Steinberg et al., 2015). Finally, the best implementation of this parameterization would require further constraining the relationship between phytoplankton biomass and $K_{1/2}$ in addition to the strength and co-variability of other drivers of zooplankton bio-geogrpahy such as temperature (Brandão et al., 2021) or the relative distribution of prey in models with multiple phytoplankton groups.

Despite the challenges, properly implementing such a parameterization could realize dramatic improvements in BGC models and our predictions of changes to marine carbon cycling. Extending from the assumption that a given optimal $K_{1/2}$ reflects the mean be-havior of a particular zooplankton community, other attributes of that community could be additionally parameterized. For instance, crustaceans associated with slower grazing (and larger $K_{1/2}$ values) are typically stronger swimmers. They tend to vertically mi-grate on daily and seasonal timescales, allowing them to actively transport carbon much faster than microzooplantkon (Steinberg & Landry, 2017). This could be represented by

increasing the flux of carbon from zooplankton into the sinking detritus pool (i.e. POC) at low $K_{1/2}$ values, without explicitly including the important role of Diel-vertical migration in carbon transport (Archibald et al., 2019). Other important BGC attributes that vary with zooplankton community composition include the recalcitrance of their detritus and thus the remineralization rates of what they contribute to export production, their sensitivity to temperature, their stoichiometry and carbon content, and their response to seasonal change in the depth of the surface mixed layer.
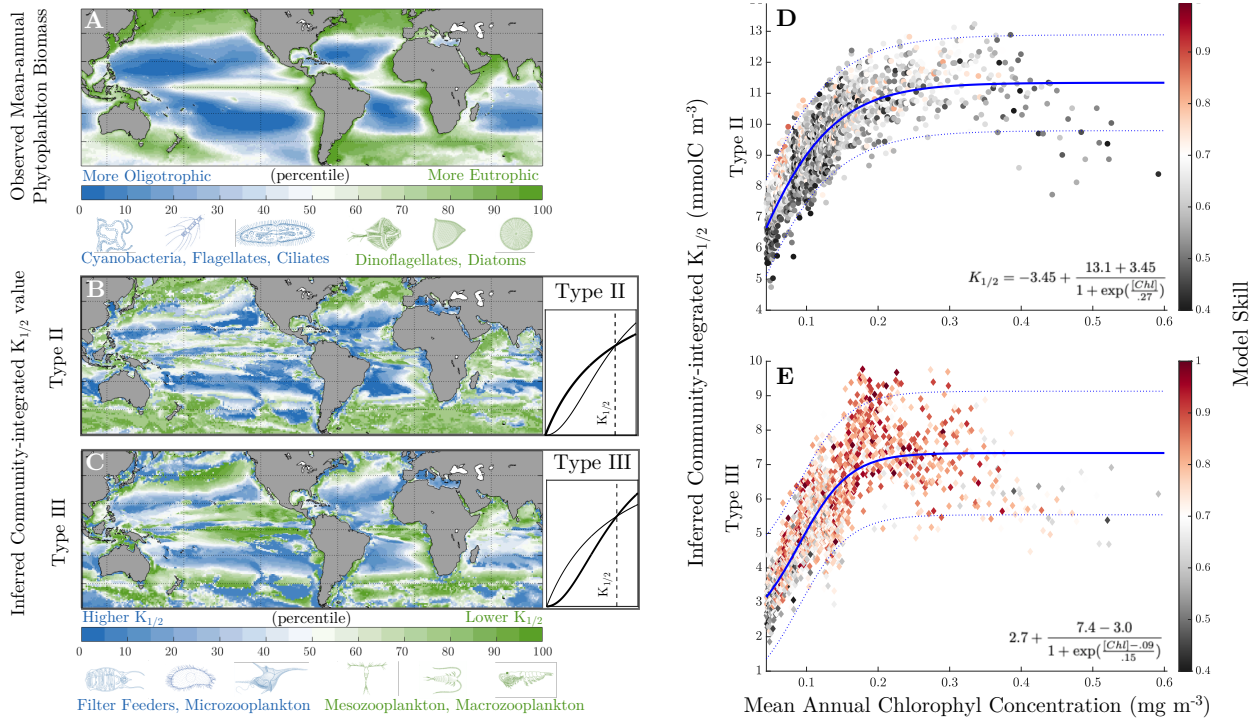
Figure S1.   Identical to **Figure 1**, except using VIIRS chlorophyll instead of CbPM

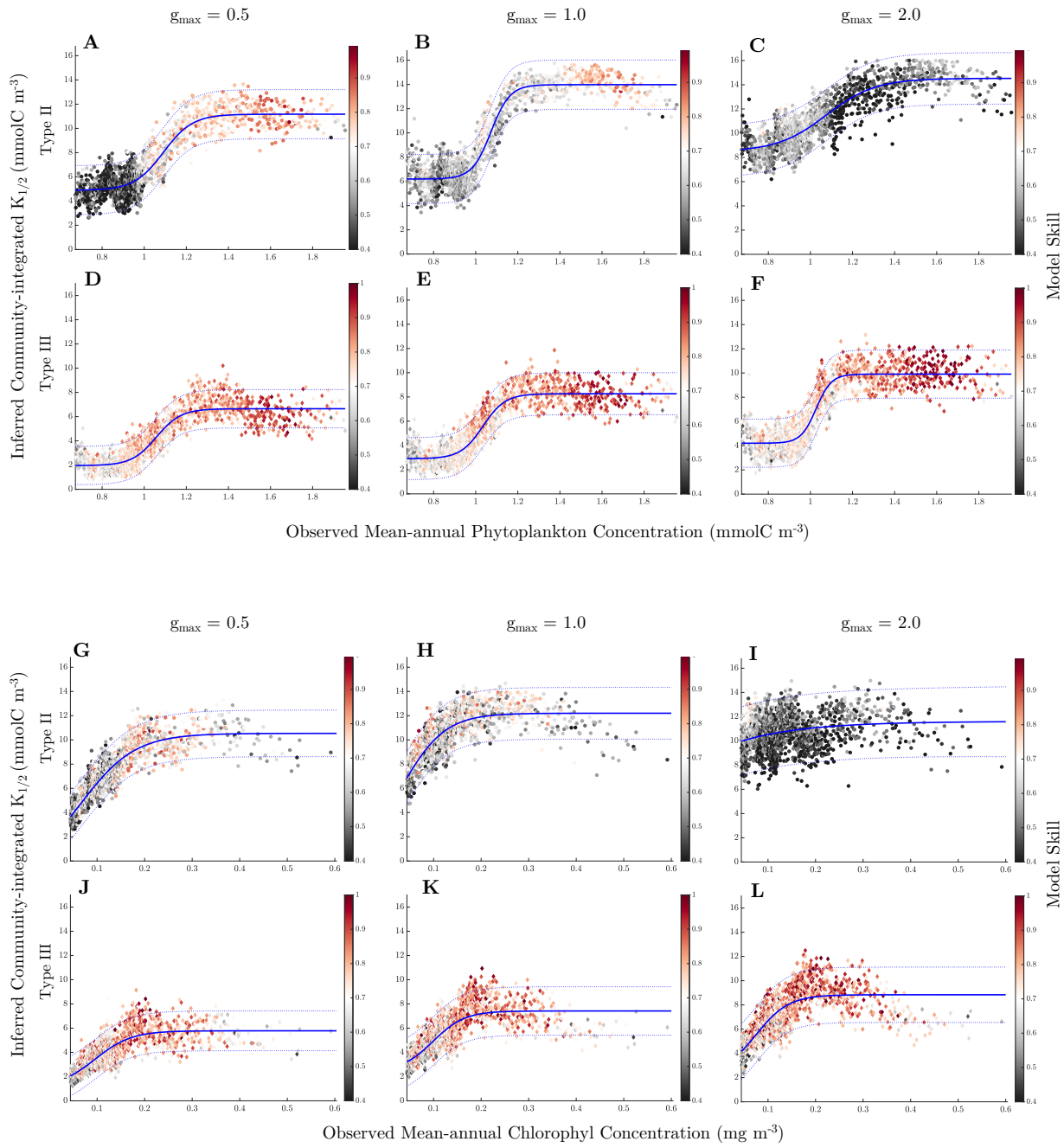carbon biomass to track the observed phytoplankton phenology.

Figure S2. Identical to **Figure 1 D, E** and **Supporting Figure 2 D, E**, expect now showing results from individual experiment suites (each using a different g_{max} value) instead of averaging optimal values across experiment suites.
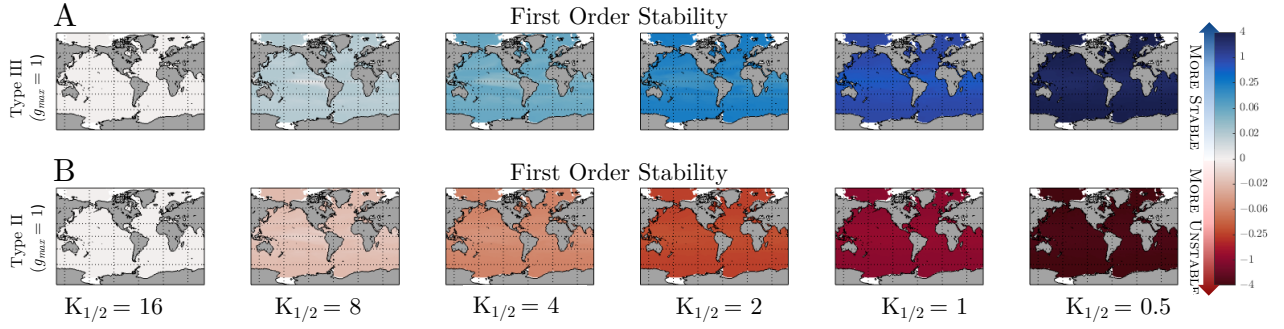
Figure S3. Sensitivity of ecosystem stability to $K_{1/2}$. Global distributions of the mean-annual first order stability is plotted for all $K_{1/2}$ values, each with a consistent $g_{max} = 1$, and a **A)** type III and **b)** type II functional response.
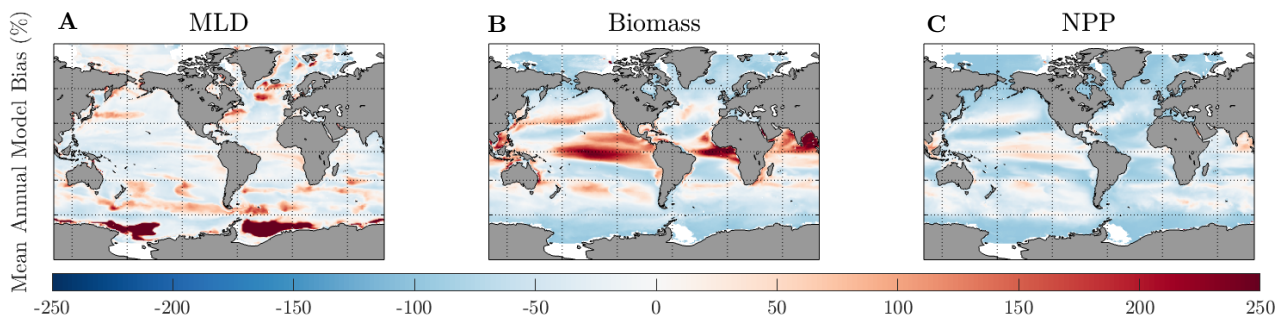
Figure S4.   The mean annual model bias is plotted for the **A)** mixed layer depth (MLD) relative to HYCOM reanalysis, **B)** Phytoplankton biomass relative to CbPM and **C)** NPP relative to CbPM.

A   Optimal $K_{1/2}$ (mmolC m⁻³) vs. Mean-annual Observed Phytoplankton Biomass (mmolC m⁻³)

Response Type	g_{max} (d⁻¹)	Parameters of Sigmoidal Fit (95% Confidence) $K_{1/2} = L + \dfrac{U-L}{1+\exp\left(\frac{[C_{phyto}]-\alpha}{\beta}\right)}$				Mean Model Skill
		L	**U**	**α**	**β**	
Type II	0.5	4.89 (4.77-5.00)	11.17 (11.05-11.29)	1.10 (1.09-1.10)	0.30 (0.28-0.33)	0.57
Type II	1	6.19 (6.10-6.28)	13.98 (13.88-14.09)	1.07 (1.06-1.08)	0.20 (0.18-0.21)	0.61
Type II	2	8.479 (8.24-8.7)	14.53 (14.36-14.69)	1.076 (1.06-1.09)	0.5 (0.45-0.57)	0.56
Type II	Mean	6.68 (6.59-6.76)	13.16 (13.07-13.24)	1.08 (1.08-1.09)	0.28 (0.27-0.30)	0.57
Type III	0.5	1.96 (1.86-2.04)	6.65 (6.57-6.78)	1.06 (1.05-1.06)	0.26 (0.23-0.28)	0.75
Type III	1	2.90 (2.80-3.00)	6.65 (8.18-8.35)	1.034 (1.03- 1.04)	0.23 (0.21- 0.25)	0.74
Type III	2	4.20 (4.11-4.29)	9.91 (9.8-10.00)	1.027 (1.02-1.03)	0.16 (0.14-0.17)	0.73
Type III	Mean	3.0 (2.92-3.10)	8.279 (8.20-8.36)	1.038 (1.03-1.04)	0.22 (0.20-0.23)	0.74

B   Optimal $K_{1/2}$ (mmolC m⁻³) vs. Mean-annual Observed Chlorophyl (mg m⁻³)

Response Type	g_{max} (d⁻¹)	Parameters of Sigmoidal Fit (95% Confidence) $K_{1/2} = L + \dfrac{U-L}{1+\exp\left(\frac{[Chl]-\alpha}{\beta}\right)}$				Mean Model Skill
		L	**U**	**α**	**β**	
Type II	0.5	-1.01 (-3.55-1.54)	10.54 (10.35-10.73)	0.06 (0.04-0.09)	0.25 (0.2102, 0.2897)	0.65
Type II	1	0.23 (-6.58-7.04)	12.2 (12.04-12.36)	12.2 (12.04-12.36)	0.20 (0.15-0.24)	0.64
Type II	2	-855 (-1.4e+06-1.48e+06)	11.61 (10.74-12.47)	-0.81 (-240-240)	0.60 (-1.14-2.34)	0.47
Type II	Mean	-3.446 (-16.04-9.15)	11.34 (11.19-11.49)	0.00 (-0.09-0.08)	0.27 (0.20-0.33)	0.59
Type III	0.5	1.10 (0.43-1.77)	5.78 (5.66-5.90)	0.10 (0.08-0.11)	0.17 (0.14-0.20)	0.79
Type III	1	2.378 (1.74-3.01)	7.42 (7.29-7.55)	0.10 (0.09-0.11)	0.15 (0.12-0.17)	0.81
Type III	2	2.28 (0.73-3.83)	8.84 (8.69-8.98)	0.08 (0.06-0.09)	0.15 (0.12-0.18)	0.85
Type III	Mean	2.00 (1.21-2.79)	7.34 (7.21-7.45)	0.09 (0.08-0.10)	0.15 (0.12-0.18)	0.82

Table S1. The relationship between mean annual phytoplankton abundance and the $K_{1/2}$ parameter required to best recreate its seasonal cycle. Different relationships refer to different response functions (II,III), g_{max} values (0.5,1,2) and observed phytoplankton variables (Carbon, Chlorophyll). Mean model skill refers to the average cost function score of the optimal $K_{1/2}$ across all grid cells in a given configuration

May 10, 2023, 6:05am